ISSN 1674-1056
http://cpb.iphy.ac.cn
http://iopscience.iop.org/cpb
中国物理 B
Chinese Physics
中国物理 Chinese Physics B

Orientation and alignment during materials processing under high magnetic fields

Zhong-Ming Ren(任忠鸣), Jiang Wang(王江), Rui-Xin Zhao(赵睿鑫)

Citation: Chin. Phys. B . 2019, 28(4): 048301. **doi:** 10.1088/1674-1056/28/4/048301
Journal homepage: http://cpb.iphy.ac.cn; http://iopscience.iop.org/cpb

What follows is a list of articles you may be interested in

Nuclear magnetic resonance measurement station in SECUF using hybrid superconducting magnets

Zheng Li(李政), Guo-qing Zheng(郑国庆)
Chin. Phys. B . 2018, 27(7): 077404. **doi:** 10.1088/1674-1056/27/7/077404

Electrical field-driven ripening profiles of colloidal suspensions

Zi-Rui Wang(王子瑞), Wei-Jia Wen(温维佳), Li-Yu Liu(刘雳宇)
Chin. Phys. B . 2018, 27(6): 068301. **doi:** 10.1088/1674-1056/27/6/068301

Generalized Drude model and electromagnetic screening in metals and superconductors

Da Wang(王达)
Chin. Phys. B . 2018, 27(5): 057401. **doi:** 10.1088/1674-1056/27/5/057401

Effect of shear on the symmetric diblock copolymer/nanorod mixture: A dissipative particle dynamics study

He Lin-Li, Zhang Rui-Fen, Ji Yong-Yun
Chin. Phys. B . 2012, 21(8): 088301. **doi:** 10.1088/1674-1056/21/8/088301

TOPICAL REVIEW — Fundamental research under high magnetic fields

Orientation and alignment during materials processing under high magnetic fields*

Zhong-Ming Ren(任忠鸣)†, Jiang Wang(王江)‡, and Rui-Xin Zhao(赵睿鑫)

State Key Laboratory of Advanced Special Steel & Shanghai Key Laboratory of Ferrometallurgy, Shanghai University, Shanghai 200444, *China*

(Received 4 December 2018; revised manuscript received 22 January 2019; published online 19 March 2019)

The characteristics of lattice structures can make crystal possess distinct anisotropic features, such as the varying magnetism in different crystal orientations and different directions. The anisotropic magnetism can also cause the free energy to vary in different orientations of crystal in a magnetic field (magnetic anisotropy energy). Magneto-anisotropy can make the crystal rotate by the magnetic force moment on the crystal with the easy axis towards the direction of the magnetic field, and can also promote the preferential growth along a certain crystal direction at the lowest energy state. By solidification, vapor-deposition, heat treatment, slip casting and electrodeposition under magnetic field, the crystal structure with high grain orientation is obtained in a variety of binary eutectics, peritectic alloys, multicomponent alloys and high temperature superconducting materials. This makes it possible to fabricate texture-functional material by using high magnetic field and magneto-crystalline anisotropy of crystal. The purpose of this article is to review some recent progress of the orientation and alignment in material processing under a high magnetic field.

Keywords: high magnetic field, orientation, alignment

PACS: 83.60.Np, 74.25.N–, 83.50.Uv, 81.30.Fb **DOI:** 10.1088/1674-1056/28/4/048301

1. Introduction

The ability to impose a preferred orientation or alignment on a crystalline material is effective in improving its physical properties. By applying a high magnetic field to a crystal, its magnetic force/torque is generated when the crystal has anisotropic magnetic properties. Table 1 shows the metallic materials aligned by a strong magnetic field.

It can be seen that both ferromagnetic and non-ferromagnetic metals can reach aligned morphologies under a sufficiently high magnetic field. From a thermodynamic viewpoint, the magnetizing of a crystal is a process involving an input of magnetization energy to the system. The magnetic energy can be expressed as follows:[12]

$$G_{\mathrm{M}} = -\int_0^{H_{\mathrm{ex}}} \mu_0 M \,\mathrm{d}H_{\mathrm{ex}}. \tag{1}$$

For a non-ferromagnetic substance, M in Eq. (1) is the volume density of magnetic dipole moment and expressed as

$$M = \chi H_{\mathrm{ex}}. \tag{2}$$

Inserting Eq. (2) into Eq. (1) yields

$$G_{\mathrm{M}} = -\int_0^{H_{\mathrm{ex}}} \mu_0 M \,\mathrm{d}H_{\mathrm{ex}} = -\frac{1}{2}\mu_0 \chi H_{\mathrm{ex}}^2, \tag{3}$$

where G_{M} is the magnetization Gibbs energy, μ_0 is the magnetic permeability ($4\pi \times 10^{-7}$ H·m^{-1}), H_{ex} (sometimes using B instead) is the imposed magnetic field, and χ is the magnetic susceptibility.

As shown in Fig. 1, the χ values of a crystal are heterogeneous in different crystal directions. Therefore, from Eq. (3), the entropy varies correspondingly. Then the difference in magnetizing entropy between crystal directions c and ab is:[12]

$$\Delta G_{\mathrm{M}}^{c-ab} = G_{\mathrm{M}}^{c} - G_{\mathrm{M}}^{ab} < 0. \tag{4}$$

This means that the decrease of free energy along the c-axis direction is more evident than the one along the ab axis. Therefore, the magnetic field enhances the growth in the c-axis direction and promotes the consequent growth alignment.

It is necessary that a critical radius should be reached for the nuclei in a liquid metal to achieve the magnetic alignment. As given in Eq. (5), the critical radius can be derived from Eq. (1) under the assumption of a spherical particle.

$$r > \sqrt[3]{\frac{3\mu_0 k_{\mathrm{B}} T}{2\pi\left(\chi_c - \chi_{a,b}\right) B^2}}, \tag{5}$$

where k_{B} is the Boltzmann constant, χ_c is the magnetic susceptibility along the c axis, and $\chi_{a,b}$ is the magnetic susceptibility along the ab axis. For instance, the critical radius for bismuth is 16.5 nm.

*Project supported by the National Natural Science Foundation of China (Grant Nos. U1560202, 51690162, and 51604172), the National Science and Technology Major Project "Aeroengine and Gas Turbine", China (Grant No. 2017-VII-0008-0102), and the Shanghai Science and Technology Project, China (Grant No. 17JC1400602).

†Corresponding author. E-mail: renzm2201@163.com

‡Corresponding author. E-mail: jiangwang417@163.com

© 2019 Chinese Physical Society and IOP Publishing Ltd

Table 1. Summary of metallic materials aligned by strong magnetic field.[1–5]

Metallic materials	Crystal structures	Magnetic flux density, T	Aligned direction	Ref.
Al-Cu alloy	Al_2Cu (paramagnetic) tetragonal	–10	c-axis$\parallel \boldsymbol{B}$	[6], [7], [8]
Cd–Zn alloy	Zn (diamagnetic) hexagonal	1	c-axis$\parallel \boldsymbol{B}$	[6]
Al–Ni alloy	Al_3Ni (paramagnetic) orthorhombic	10	c-axis$\parallel \boldsymbol{B}$	[6], [9]
Al–Mn alloy	Al_6Mn (paramagnetic) orthorhombic	10	c-axis$\parallel \boldsymbol{B}$	[10]
Mn–Bi alloy	$Mn_{1.08}Bi$ (paramagnetic) hexagonal	10	c-axis$\parallel \boldsymbol{B}$ >Curie temperature	[11]
	MnBi (ferromagnetic) hexagonal	0.5	c-axis$\parallel \boldsymbol{B}$ >Curie temperature	
Bi, Bi–Sn alloy	Bi (diamagnetic) hexagonal	5, 12	c-axis$\perp$B	[12]
Mn–Sb alloy	MnSb (paramagnetic) hexagonal	12	c-axis$\parallel \boldsymbol{B}$ >Curie temperature	[1]
Sm–Co	Sm_2Co_{17} (paramagnetic) hexagonal	2.5	c-axis$\parallel \boldsymbol{B}$ >Curie temperature	[4]
Al–Fe	Al_3Fe (paramagnetic) monoclinic	12	$\langle 543\rangle \parallel \boldsymbol{B}$	[2]
Nd–Fe–B alloy	$Nd_2Fe_{14}B$ (paramagnetic) tetragonal	5	c-axis$\parallel \boldsymbol{B}$ >Curie temperature	[3]
Co–Sn alloy	Co primary phase (paramagnetic) hexagonal	3, 12	Co dendrite$\parallel \boldsymbol{B}$ >Curie temperature	[5]
Alignment due to shape anisotropy				
Al–Si–Fe alloy	Al-9 wt%Si–15 wt%Fe (needle shape)	5	long direction of the crystal$\perp \boldsymbol{B}$	[12]
Alignment during vapor-deposition				
Bi film	vapor-deposition	5	c-axis$\perp \boldsymbol{B}$	[10]
Zn film	vapor-deposition	6	c-axis$\parallel \boldsymbol{B}$	

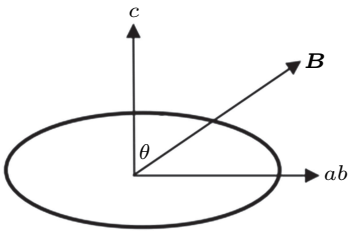


Fig. 1. Anisotropic grain in magnetic field, where B is magnetic field direction. c and ab are crystallographic axes, respectively.[6]

According to the theory of magnetic anisotropy, it is not necessary for the crystal to have a non-cubic structure. However, it is more common for non-ferromagnetic materials with non-cubic crystal structures to achieve the magnetic alignment. In some cases, magnetic alignment can also be induced by the shape magnetic anisotropy due to the shapes of the crystals, for instance, the needle-like phases precipitated from a liquid metal. Because of the shape anisotropy, the particle is aligned along the direction with a lower system energy imposed by the anisotropic demagnetizing field. It can be expressed in Eq. (6) as follows:

$$\Delta U \propto \left(B^2/2\mu_0\right)\left(\chi_{\mathrm{P}}^2-\chi_{\mathrm{M}}^2\right)\left(N_{\perp}-N_{\parallel}\right), \tag{6}$$

where $\Delta U = U_{\perp} - U_{\parallel}$ indicates the difference in magnetic energy between the particle aligning perpendicular and that parallel to the magnetic field direction; χ_{P} and χ_{M} are the magnetic susceptibility of the particle and liquid metal, respectively; $N_{\perp}$ and $N_{\parallel}$ are the demagnetizing coefficient perpendicular and parallel to the needle axis of the particle. The value of $N_{\perp}$ is larger than that of $N_{\parallel}$ in the most cases for the particle with a needle-like shape, such as a primary dendrite arm. Therefore, if $\chi_{\mathrm{P}} > \chi_{\mathrm{M}}$, $\Delta U > 0$ and the particle should be parallel to the imposed magnetic field direction. If $\chi_{\mathrm{P}} < \chi_{\mathrm{M}}$, $\Delta U < 0$ and the particle aligns perpendicularly to the magnetic field.[10,12]

There are several ways to achieve magnetic alignment during the processing of metallic materials, such as solidification, vapor-deposition, heat treatment, slip casting and electrodeposition.

2. Reviews of researches on orientation and alignment in processing various materials

In 1981, Mikelson and Karklin first obtained the aligned solidification structure in Al–Ni, Al–Cu, Bi–Cd, and Cd–Zn

alloys under a 0.5 T–1.5 T magnetic field.[6] Subsequently, Savitsky *et al.* found that the primary MnBi ferromagnetic crystal phase in Bi-(0.9–10) wt%Mn alloys aligned along the direction of a magnetic field of 2.5 T during solidification (see Fig. 2).[11] De Rango *et al.* first prepared the bulk texture of $YBa_2Cu_3O_7$ superconductor in solidification process under a high magnetic field of 5 T.[13] Katsuk reported that the diamagnetic benzophenone crystallized from n-hexane, KCl and $BaCl_2$ crystallized from solution aligned under a 10-T magnetic field.[14] Texture crystal growth of Bi-2201 and Bi (Pb) 2212 have been also obtained under a high magnetic field. Asai put forth the perpendicular alignment of the primary phase during solidification of Al–Si–Fe alloy under a strong magnetic field of 5.5 T.[15]

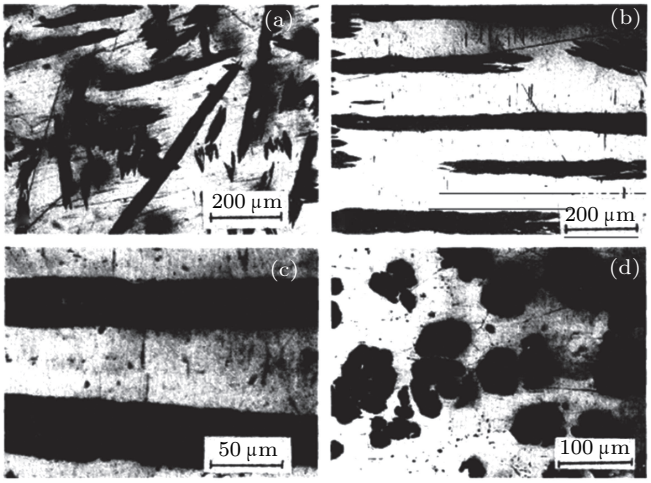


Fig. 2. Microstructures of Bi–10 wt%Mn alloy: (a) crystallization without external magnetic field; (b) and (c) cross-section parallel to applied magnetic field; (d) cross-section normal to applied magnetic field.[11]

Thashi *et al.* also achieved the crystal alignment in vapor deposition process by using a high magnetic field. As shown in Fig. 3, the zinc crystals were found to be oriented to the easy magnetic axis parallel to the magnetic direction in resistance method.[16]

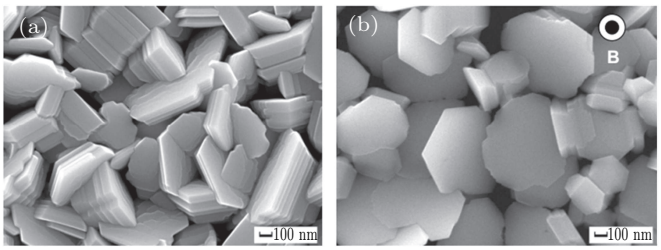


Fig. 3. Zn film obtained by vapor-deposition without (a) and with (b) 6-T magnetic field.[16]

The crystal alignment during the solid phase transformation was also found under a high magnetic field. The first observation of aligned microstructures in steels was made on Fe–0.1%C and Fe–0.6%C alloys undergoing α-to-γ transformation in a magnetic field of 8 T.[17] The chain or columnar γ phase was developed along the magnetic field in the matrix of α phase as shown in Fig. 4. The formation mechanism of the aligned structure is attributed to the dipolar interaction between the nuclei of γ phase regarded as magnetic holes in the background of ferromagnetic medium of α phase. Subsequently, the same author successfully achieved an aligned microstructure during the austenite-to-ferrite transformation in steels under a magnetic field of 12 T. At the same time, the formation mechanism of the aligned structures was discussed from the viewpoint of the nucleation and growth of ferrite grains in austenite phase under a magnetic field.

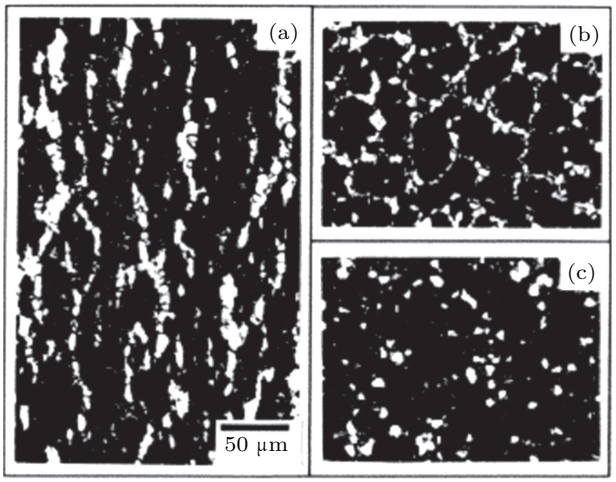


Fig. 4. Microstructures of Fe–0.6 wt%C specimens kept at 745 °C for 45 min: (a) cross-section parallel to magnetic field 8 T; (b) cross-section perpendicular to the field; (c) under the same treatment in zone magnetic field.[17]

In China, the relevant researches have been extensively carried out since the beginning of this century, which can be marked by the first paper published by the researchers from Shanghai University in 2002. The research group headed by Zhong-Ming Ren in Shanghai University mainly focused on the orientation and alignment behaviors of metals in the solidification process. They systemically studied the alignment of MnBi phase in the Bi–Mn alloy and its morphology evolution rule during the bulk solidification under different intensities of magnetic field.[18–24] By maintaining the melt at a constant temperature (above or below the curie temperature of Bi–Mn alloy) in different times, they analyzed the alignment and growth dynamics of the MnBi phase. In the mushy zone orient, the MnBi crystals congregated and grew up preferentially along the direction of the applied magnetic field in the Bi–Mn alloys solidification process. Besides the Bi–Mn system, they also verified the orientation effect of the static magnetic field on the Al–Ni[9] and Al–Cu[7,8] system and found that the $A1_3Ni$ crystal orientation and the *c* plane of $A1_3Ni$ crystal alignment are perpendicular to the direction of magnetic field. For the Al–Cu system, they pointed out that the alignment structure was formed and the $\langle 111 \rangle$ crystal direction turned to the direction of the magnetic field during directional solidification of the Al–4.5 wt%Cu alloy with a grains

growth speed of 50 μm/s and thermal gradient of 3800 K/m. It should be noticed that they in fact began to use the forced solidification method to enhance the alignment effect on solidification of metals with assistance of the static magnetic field in 2005. For the directional solidification of Bi–Mn alloy, they reported that the high magnetic field has enhanced the formation speed range of MnBi fiber and regularized the MnBi/Bi eutectic structure. As shown in Fig. 5, the average spacing and diameters of MnBi fibers increased under the magnetic field.[24] The addition of high magnetic field made the arrangement of directionally solidified microstructure more regular. Obviously, the MnBi fiber began to coarsen and the fiber spacing increased. With the rise of magnetic field intensity, the small facet growth characteristics were enhanced.

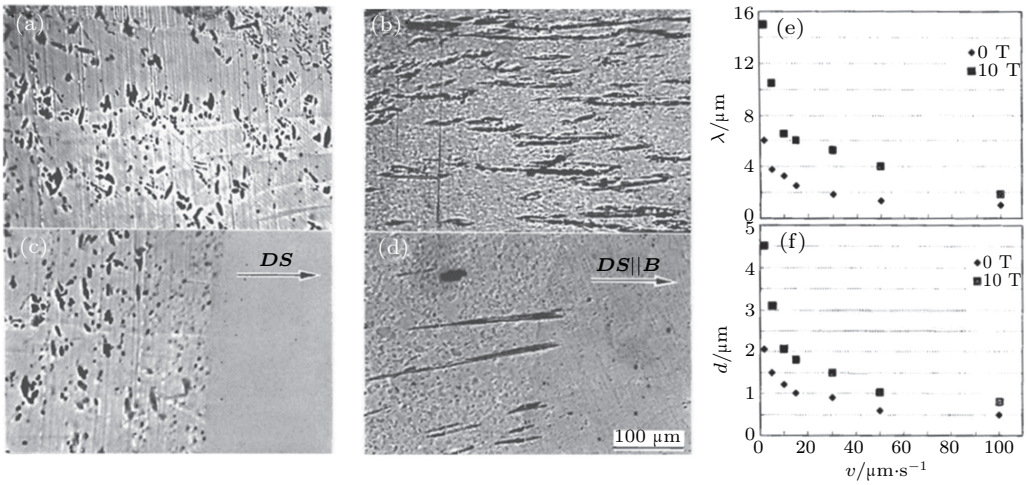


Fig. 5. Influence of magnetic field on directional solidification structure, (a) and (b): without magnetic field; (c) and (d): with 2-T magnetic field; evolution of average spacing (e) and average diameter (f) with growth velocity under different magnetic fields.[24]

Except for the single phase and eutectic alloys, the alignment of the monotecitc alloys can also be realized by using high static magnetic field during their solidification. In 2008, Wang *et al.* reported that some of aligned solidification structures were formed in the alloys of Fe–49 wt%Sn and Cu–40 wt%Pb under a high magnetic field.[25] They attributed such structures to the difference in magnetic anisotropy energy between α-Fe crystal orientation and the preferential growth of α-Fe dendrite; in the Cu–40 wt%Pb alloy under a 12-T high magnetic field, the motion of Pb-rich droplets and the molten flow in the solidifying front was suppressed by the external field, which indicates the formation of much longer, regularly aligned rod-like Pb-rich phase in the center of sample. More recently, Zhong *et al.* also found the aligned structure of Bi–5 wt%Zn formed during solidification under various high magnetic fields as shown in Fig. 6;[26,27] the *c* axis of Zn crystal in the eutectic BiZn structure is the maximum magnetic susceptibility, which be aligned parallel to the direction of 6-T high static magnetic field completely. Both Wang and Zhong considered that such an aligned structure was formed in two steps: the minor phase droplets' movements were first damped by the high magnetic fields and then grown in a certain direction.

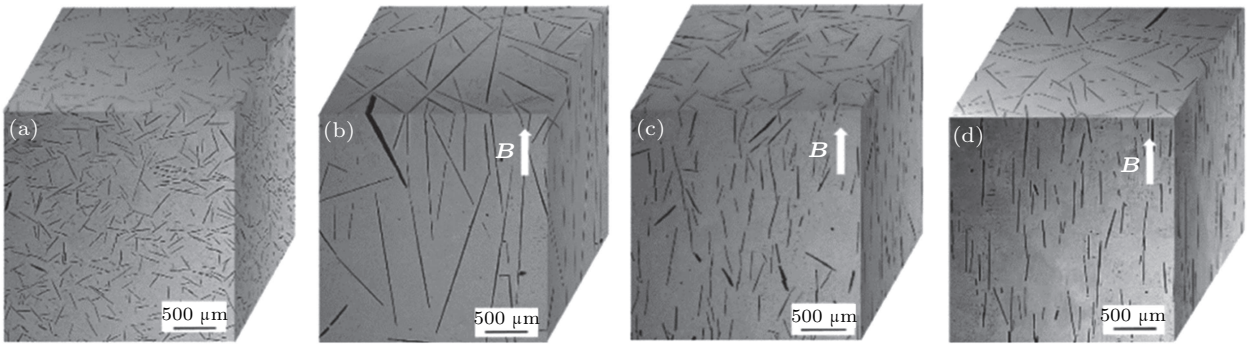


Fig. 6. Three-dimensional microstructures of Bi–5 wt% Zn immiscible alloys solidified under various magnetic fields: (a) 0 T, (b) 2 T, (c) 4 T, (d) 6 T.[27]

Heat treatment is also another important materials processing technique, during which the texture is desired for most cases. A research group of Northeastern University is most active in this field in China. They first studied the effect of magnetic field intensity on the microstructure of proeutectoid ferrite in Fe–0.12%C[28] and Fe–0.76%C alloy.[29] It was found that the proeutectiod ferrite grains were elongated along the magnetic field direction, and the angle between the major axis of proeutectoid ferrite and magnetic field direction decreased with magnetic field intensity increasing.[29] They ex-

plained such an observation as follows: the proeutectoid ferrite becomes the magnetic dipolar under high magnetic field, and then the diffusion of polarized austenite atoms is easier to form the ferrite grain along the magnetic field direction. In 2013, Wang *et al.* reported their work on the effect of magnetic field on crystal orientation, morphology and magnetostriction of $TbFe_2$ and $Tb_{0.27}Dy_{0.73}Fe_{1.95}$ alloys in heat treatment process.[30] They found that high magnetic field did not change the orientation of the R–Fe alloy, but the orientation degree had a great improvement after heat treatment.

It can be seen that the aligned structure is more favored by the functional materials. The chemical synthesis (electrodeposition), vapor-deposition and slip casting are the most important fabricating methods. In such processes, the alignment effect of high static magnetic field works as well. In 2007, Ren *et al.* found that the one-dimensional growth of the nano-sized cobalt ferrite was enhanced by a 10-T static magnetic field in the synthesis process.[31] Three years later, they also confirmed that the magnetic field can align with the Zn crystal during the film fabrication. They achieved the Zn film growth via the vacuum evaporation method and found that the preferential growth direction of such a film was strongly affected by a strong magnetic field.[32] Wang *et al.* investigated that the influence of Co doping on the orientation behavior of ZnO film during fabrication under a magnetic field.[33] They found that a 6-T magnetic field can give rise to the formation of rod-like ZnO grains, and the preferred orientation of (101) transforms to that of (002) with oxidation time increasing under a high magnetic field. Very recently, a paper in this field was published by the high magnetic field laboratory of Chinese Academy of Sciences. Xu *et al.* studied the influence of high magnetic field on the molecular orientation and the morphology of iron phthalocyanie thin film. It was found that in the presence of the external magnetic field, the deposited FePc film showed a higher crystallinity and slightly closer packing in the (002) plane than those without magnetic field. Figure 7 shows the x-ray diffraction spectra of FePc thin films grew without and with magnetic field.[34] In 2010, Ma *et al.* fabricated the GdBCO bulks under a strong magnetic field and a textured structure was found under a 10-T magnetic field.[35] Such a texture structure favors the superconductivity property of the sample.

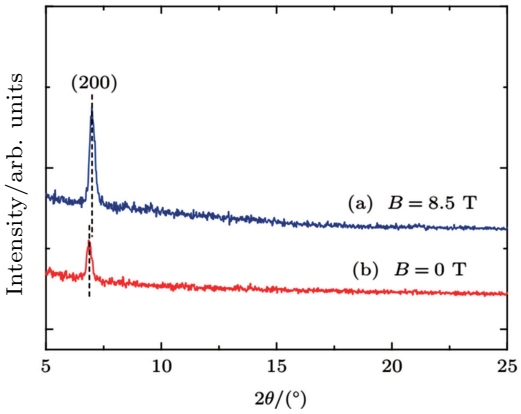


Fig. 7. X-ray diffraction spectra of FePc thin films grown without (a) and with (b) magnetic field.[34]

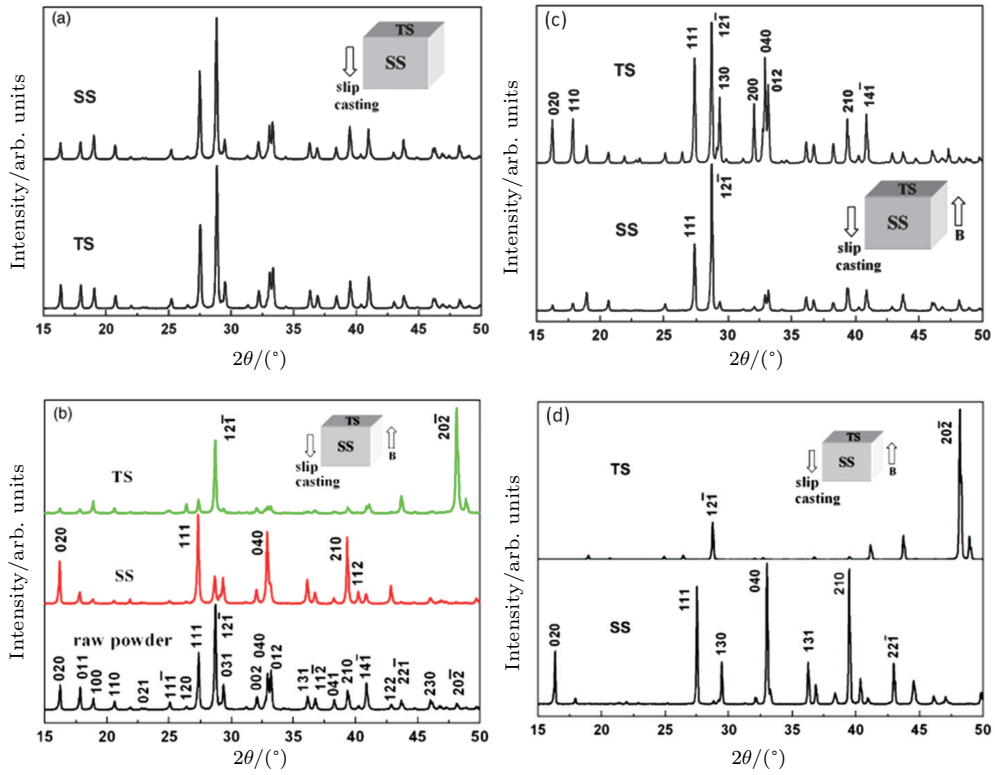


Fig. 8. X-ray diffraction patterns of green bodies prepared (a) without and (b) with a strong magnetic field of 12 T, and those are collected on the top and side surfaces of samples sintered at 1350 °C for 90 min in air. X-ray diffraction patterns of (c) 0-T sample; (d) 12-T sample.[36]

For the ceramics, slip casting is the main manufacturing method. The texture structure can be obtained by applying high magnetic field to this process, and in fact such an aligned structure is desired for some ceramics. In this field, the first research in China was carried out by Zhou *et al.*[36] They tried to clip the texture of γ-$Y_2Si_2O_7$ with the assistance of high magnetic field in the two-step sintering process. They used a high magnetic field in the slip casting process and found that the texture obtained in the green bodies could be preserved after sintering. Figure 8 shows the XRD patterns of their green bodies obtained by slip casting under magnetic field and the corresponding sintered samples.

Zhang *et al.* fabricated highly textured ZrB_2-based ultra-high temperature ceramics via strong magnetic field alignment in 2009.[37] And recently, Pan *et al.* prepared a grain-oriented structure CeF_3 ceramic by imposing a high magnetic field in its slip casting process.[38]

3. Conclusions

In summary, it is not difficult to find that the orientation and alignment effect of high magnetic field has been widely accepted and applied to various material processes to obtain the texture structure. In this field, Chinese scientists have conducted extensive and in-depth researches. It can be found that the high static magnetic field is still a powerful method to control the crystal and grain orientation, and it can be expected to possess more practical applications in the future.

References

[1] Wang Q, Liu T, Zhang C, Gao A, Li D and He J 2009 *Sci. Technol. Adv. Mater.* **10** 1
[2] Han Y, Ban C, Guo S, Liu X, Ba Q and Cui J 2007 *Mater. Lett.* **61** 983
[3] Rivoirard S, Barthem V M T S, Garcin T, Beaugnon E, De Miranda P E V and Givord D 2009 *J. Phys.: Conf. Ser.* **156** 012009
[4] Legr, B A, Chateigner D, Perrier De La Bathie R and Tournier R 1998 *J. Alloys Compd.* **275–277** 660–664
[5] Wang J, Li J, Hu R, Kou H and Beaugnon E 2015 *Mater. Lett.* **139** 288
[6] Mikelson A E and Karklin Y K 1981 *J. Cryst. Growth* **52** 524
[7] Li X, Ren Z, Fautrelle Y, Zhang Y and Esling C 2010 *Acta Mater.* **58** 1403
[8] Li X, Ren Z, Sun Y, Wang J, Yu J and Ren W 2006 *Acta Metall. Sin.* **42** 147
[9] Li X, Ren Z, Wang H, Deng K and Xu K 2006 *Chin. J. Nonferrous Met.* **16** 476
[10] Zhang W and Dou Y 2009 *Mater. Mech. Eng.* **33** 18
[11] Savitsky E M, Torchinova R S and Turanov S A 1981 *J. Cryst. Growth* **52** 519
[12] Yamguchi M and Tanimoto Y 2006 *Magneto-Science Magnetic Field Effects on Materials: Fundamentals and Applications* (Springer)
[13] de Rango P, Lees M, Lejay P, Sulpice A, Tournier R, Ingold M, P Germl M P 1991 *Nature* **349** 770
[14] Akio Katsuki, Ryoko Tokunaga S W and Y T 1996 *Chem. Lett.* 607–608
[15] Morikawa H, Sassa K and Asai S 1998 *Mater. Trans. JIM* **39** 814
[16] Tahashi M, Ishihara M, Sassa K and Asai S 2003 *Mater. Trans.* **44** 285
[17] Shimotomai M and Maruta K 2000 *Scr. Mater.* **42** 499
[18] Wang H, Ren Z, Deng K and Xu K 2002 *Acta Metall. Sin.* **38** 41
[19] Wang H, Ren Z, Deng K and Xu K 2002 *Chin. J. Nonferrous Met.* **12** 556
[20] Wang H, Zhong-Ming R, Li X, Li W, Deng K and Xu K 2003 *Trans. Nonferrous Met. Soc. Chin.* **13** 1405
[21] Zhang B, Ren Z, Wang H, Li X and Zhuang Y 2004 *Acta Metall. Sin.* **40** 604
[22] Li X, Ren Z, Wang H, Li W, Deng K and Zhuang Y 2004 *Acta Metall. Sin.* **40** 40
[23] Li X, Ren Z, Yu J, Wang H and Deng K 2005 *Acta Metall. Sin.* **41** 685
[24] Li X, Ren Z, Deng K, Zhuang Y and Xu K 2005 *Acta Metall. Sin.* **41** 588
[25] Wang E, Zuo X, Zhang L and He J 2008 *Sprcial Casting & Nonferrpis Aalloys*, Vol. 04 pp. 478–481
[26] Zhong Y, Wang J and Zheng T X 2012 *Journal of Iron Steel Research, International* pp. 283–285
[27] Zheng T, Zhong Y, Lei Z, Ren W, Ren Z, Wang H, Wang Q, Debray F, Beaugnon E and Fautrelle Y 2015 *Mater. Lett.* **140** 68
[28] Song J, Zhao X, Wang S, Gong M and Zuo L 2008 *Acta Metall. Sin.* **44** 1305
[29] Gong M, Zhao X, Wang S and Zuo L 2008 *Acta Metall. Sin.* **44** 615
[30] Liu Y, Liu T, Wang Q, Wang H, Wang L and He J 2013 *Acta Metall. Sin.* **49** 1148
[31] Gui L, Zhong Y, Fu X, Lei Z and Ren Z 2007 *Acta Metall. Sin.* **43** 529
[32] Ren S, Ren Z and Ren W 2010 *J. Vac. Sci. Technol.* **30** 430
[33] Li G, Wang H, Wang Q, Zhao Y, Wang Z, Du J and Ma Y 2015 *Nanoscale Res. Lett.* **10** 1
[34] Huang C, Liu L, Fang J, Zhang W, Wang K, Gao P and Xu F 2016 *Acta Phys. Sin.* **65** 156101 (in Chinese)
[35] Wang L, Ma Y, Wang D, Wang J, Satoshi A and Kazuo W 2010 *Chin. J. Low Temp. Phys.* **32** 127
[36] Sun Z Q, Zhu X W, Li M S, Zhou Y C and Sakka Y 2008 *J. Am. Ceram. Soc.* **91** 2521
[37] Ni D, Zhang G, Kan Y and Sakka Y 2009 *Scr. Mater.* **60** 615
[38] Li W, Sun Y, Kou H, Chen M, Shi Y, Feng X, Pan Y and Guo J 2014 *Ceram. Int.* **40** 10317